INL/EXT-14-33601

Light Water Reactor Sustainability Program

Irradiation Programs and Test Plans to Assess High-Fluence Irradiation-Assisted Stress Corrosion Cracking Susceptibility of Stainless Steels

November 2014

U.S. Department of Energy

Office of Nuclear Energy

INL/EXT-14-33601

Irradiation Programs and Test Plans to Assess High-Fluence Irradiation-Assisted Stress Corrosion Cracking Susceptibility of Stainless Steels.

S. Teysseyre

November 2014

Prepared for the
U.S. Department of Energy
Office of Nuclear Energy

Abstract

Irradiation-assisted stress corrosion cracking (IASCC) is a known issue in current nuclear reactors. In a 60-year lifetime, reactor core internals may experience fluence levels up to 15 dpa for boiling water reactors (BWRs) and 100+ dpa for pressurized water reactors (PWRs). To support safe operation of our fleet of reactors and maintain their economic viability, it is important to be able to predict any evolution of material behaviors as reactors age and, therefore, as fluence accumulated by reactor core components increases. For PWRs, the difficulty to predict high-fluence behavior comes from the fact that there is not a consensus about the mechanism of IASCC and that little data are available. However, it is possible to use the current state of knowledge on the evolution of irradiated microstructure and on the processes influencing IASCC to emit hypotheses. This report identifies several potential changes in microstructure and proposes to identify their potential impact on IASCC. The susceptibility of a component to high-fluence IASCC is considered to depend on the intrinsic IASCC susceptibility of the component due to radiation effects on the material, as well as be related to the evolution of the loading history of the material and interaction with the environment as total fluence increases.

To address the lack of IASCC propagation and initiation data generated with material irradiated in a PWR condition, it is proposed to investigate the validity of generating high-fluence materials by adding fluence to a pre-existing irradiated microstructure. A long-term irradiation that is aimed at generating materials with a well-controlled irradiation history is also proposed for consideration. Single variation-type experiments are proposed with materials that are representative of PWR conditions and with materials irradiated in other conditions.

For BWRs, the study of available data permitted identification of an area of concern for the long-term performance of a component exposed to high fluence: the efficiency of hydrogen water chemistry mitigation technology may decrease as fluence increases for high-stress intensity factors. This report describes a program plan to determine the efficiency of hydrogen water chemistry as a function of the stress intensity factor applied and the fluence. The use of existing, available materials and the generation of additional materials via irradiation in a research reactor are considered.

CONTENTS

FIGURES

TABLES

ACRONYMS

ASTM	American Society of Testing and Materials
ATR	Advanced Test Reactor
BWR	boiling water reactor
CGR	crack growth rate
CT	compact tension
EPRI	Electric Power Research Institute
HAZ	heat affected zone
HFIR	High-Flux Isotope Reactor
HWC	hydrogen water chemistry
IASCC	irradiation- assisted stress corrosion cracking
K	stress intensity factor
NWC	normal water chemistry
PWR	pressurized water reactor
TEM	Transmission Electron Microscope
YS	yield strength

Irradiation Program and Test Plans to Assess High-Fluence Irradiation-Assisted Stress Corrosion Cracking Susceptibility of Stainless Steels

1. INTRODUCTION

As commercial nuclear power plants age and as reactor internal components accumulate high fluence, there is a legitimate concern that component failure by an irradiation-assisted stress corrosion cracking (IASCC) mechanism may increase. An increase in the number of failures may be due to an increase of components reaching a "threshold" for IASCC, an increase of the intrinsic susceptibility of the materials, or a combination of events (e.g., aging, fatigue, differential loading, etc.) that initiate cracking in a susceptible material.

This report proposes irradiation test plans and test matrices to address the concern of material performance at high fluence with regard to IASCC for pressurized water reactors (PWRs) and boiling water reactors (BWRs). The approaches proposed include generation of a specific set of specimens to directly measure the IASCC susceptibility of the material as dose increases for the reactor of interest and experiments designed to study specifics aspects of IASCC susceptibility or to quantify the influence of a particular parameter on IASCC.

2. HIGH-FLUENCE IRRADIATION-ASSISTED STRESS CORROSION CRACKING FOR PRESSURIZED WATER REACTOR MATERIALS

2.1 Introduction

2.1.1 Background

For PWRs, in-core components are expected to reach 100+ dpa by the end of their currently planned lifetime. Literature review (Chopra2011, Lian 2013, Rao 2008, Rao 2009, Tang 2003, Tang 2005) indicates that most of the studies on IASCC in PWR environment have been conducted on BWR-irradiated materials or fast reactor materials. Studies on PWR materials at high fluences are limited and crack initiation data available to the public are limited to doses below 38 dpa. However, from the limited studies available, we can capture a behavior at odds with our current understanding of IASCC where crack growth rates (CGRs) of austenitic stainless steel material irradiated in a PWR to about 38 dpa show no environmental enhancement of growth rates and CGRs of the irradiated material are comparable to those of unirradiated materials. Crack initiation data are available for higher doses (i.e., 70 dpa), but they are limited (Freyer 2007). There is a need for data generated with materials irradiated in PWR relevant conditions. Without such materials, an attempt to predict IASCC has to rely on the current understanding of low and intermediate fluence IASCC and on an estimate of the evolution of the microstructure, which are summarized as follows:

- Radiation-induced segregation is not seen as an issue for IASCC in PWR environments due to the low corrosion potential. Because this phenomenon saturates quickly for the major elements (Cr), it is usually not seen as a rising issue as high fluence accumulates. However, there is potential for enrichment in silicon that could lead to increased IASCC susceptibility due to the solubility of silicon (Andresen 2004, Andresen 2005). It also was suggested (Garner et al. 2006) that radiation-induced segregation along free surfaces (e.g., grain boundaries and bubble walls) may lead to significant changes in local composition that could lead to a local increase in ferrite and a modified dislocation structure.
- Hardening is an important parameter for stress corrosion cracking. Radiation-induced hardening increases IASCC susceptibility; however, the effect of radiation hardening on crack propagation

seems be to saturate. Therefore, it is not expected to change fluence increases. However, the mode of deformation of a hardened microstructure (due to the dislocation structure and vacancies) leads to localization of the deformation into channels (localization is believed to be an important factor for stress corrosion cracking). The presence of irradiation-induced precipitation may further influence hardening at high fluence and, thus, influences local deformation.

- Swelling will occur at the highest temperatures observed in a PWR. Swelling can be a consequence of the presence of voids and bubbles, both intergranularly and intragranularly. Currently, there has been no indication that swelling will influence the propagation of IASCC cracks; however, no attempt to directly quantify such effect was identified. Swelling will affect fracture toughness. It is commonly accepted that the main role of swelling on IASCC will be to increase the stress applied to components such as baffle bolts. This effect will be balanced by radiation stress relaxation. However, radiation creep can help sustain stress corrosion cracking as it promotes dynamic strain, which has a strong effect on stress corrosion cracking.
- Finally, other factors may emerge at very high fluence.

High-fluence IASCC can be approached from two different angles. The first approach is to focus on the evolution of the microstructure of the material as accumulated fluence rises and to study the susceptibility of this microstructure to IASCC. This approach requires generating materials that are either representative of the materials present in the field or materials that exhibit features that will appear in those materials (e.g., precipitation or swelling) and whose impact on IASCC (e.g., initiation and propagation) must be studied. Another approach consists in having a more holistic approach of IASCC and accounting for the fact that IASCC may be observed at high fluence, not as a consequence of an increase of IASCC susceptibility of the material itself, but because other phenomena created the precursors for IASCC initiation. For instance, stress relaxation will relieve the stress initially applied to components and would decrease the probability of crack initiation. However, swelling may reload the specimen and radiation creep could promote crack initiation by applying a sustained dynamic strain. Work performed on the influence of the strain path on stress corrosion cracking initiation in a PWR environment (Couvant 2004, Couvant 2009, Couvant 2011) suggests that a change of the strain path has a significant impact on the susceptibility of stainless steel and nickel alloys to intergranular SCC while reloading the specimen. More generally heterogeneous deformation may have a significant effect of cracking. This is allegedly due to strain localization induced by an orthogonal strain path (Schmitt 1985). This effect could be active when baffle bolts are reloaded by swelling or deformed by irradiation creep. The loading history of baffle bolts due to swelling and irradiation creep history is addressed by the Electric Power Research Institutes (EPRI) (MRP-135, MRP-211) and will be calculated for each specific reactor. The role of the component's loading history in the initiation of IASCC in irradiated material is generic and should be studied. This work investigates the role of the initial microstructure as a precursor of IASCC initiation. Another phenomenon that may generate a precursor condition for IASCC is fatigue loading of the component. As fluence increases, hardening will increase. Precipitations and swelling may affect hardening and strain localization and therefore may affect fatigue resistance of the component but may also generate the precursor for IASCC initiation. Similarly, favorable conditions for martensitic transformation and the increased hydrogen content in the material may lower the component's resistance to IASCC initiation.

This report proposes different research plans that will lead to a better understanding of high-fluence IASCC and/or generate the material needed for such research, including the following:

- An irradiation program that would generate high-fluence specimens for IASCC initiation and propagation studies and characterization of microstructure evolution
- An irradiation program and test plan to address the influence of flux and spectrum on material microstructure to assess the validity of irradiation of harvested components

- An experiment plan to address the role of heterogeneous deformation on IASCC initiation
- An experiment plan to address the role of hydrogen on IASCC initiation and propagation
- An experiment plan to address the role of swelling on IASCC propagation.

2.1.2 Limitations of this Report

Some of the initial objectives of this report were to identify the needs of specimens to address the issues of IASCC for high-fluence materials, select the reactors available for generating the material needed, designing irradiation, and determining the cost associated with irradiation. While working on this report, it became clear that a significant amount of uncertainties were associated with this work, including uncertainties in the ability of the given reactor to operate in a stable condition for a long period of time; uncertainties about the actual duration of the irradiation (i.e., considering the cost associated with irradiation and the will of the reactor operators to commit so much time for one program); and uncertainties about the viability of an expensive and long-term program, including access to foreign reactors (for instance the reactor Jules Horowitz in France may become available, while others may not be suitable for a long-term partnership due to political issues). The irradiation program would need to be a collaborative effort and flexibility would need to be part of the execution. In the United States, collaboration with user facilities may permit facilitation of such an irradiation program. For this report, it was decided to use the Advanced Test Reactor (ATR) in its current configuration to plan the recommended irradiation. This was done without consideration for timing issues or funding availability.

The work presented in this report was planned only with the materials that are known to be available. The availability was verbally confirmed even if, in some cases, details about the materials are not written in the report to respect the desire of the owner of the material to not identify it publicly. More materials were identified as suitable for the work proposed but, as their availability was not confirmed, the use of these materials was not described in this report. However, it is expected that the owners of the material will be willing to participate if the activities proposed were to be initiated. Similarly, when material was available for the activity, but its form would require technique development to perform the experiment, the material is not included. As a consequence, the report presents different tasks using the same material and does not account for the fact that if the material is limited, the tasks may not be achievable concomitantly.

2.2 Program Plans

As indicated previously, most of the studies on PWR IASCC have been conducted on BWR-irradiated materials or fast reactor materials and studies on PWR materials at high fluences are limited. The obtained CGRs show significant variability; this variability could be due to the difference in irradiation temperature, in neutron spectrum, or to variability in the heat of materials. Although fast reactor data can be very useful, particularly in parametric studies, comparative PWR data and a better understanding of the relevance of comparing IASCC data from materials irradiated with different neutron flux and spectrum are needed if one is to apply data generated from fast reactors to predict the materials' response in LWRs. CGR data up to 55 dpa have been generated; however, they are proprietary data and are not accessible to the public. Therefore, it is proposed to investigate the validity of using reactors with different spectrum and flux to generate materials for the study of high-fluence IASCC in PWRs and to initiate a long-term irradiation program that will irradiate the same heats of material from 0 to 60 dpa. Investigation of the effect of spectrum and flux would allow determination if faster and more economical ways for generating needed materials are available. The long-term irradiation program would offer the possibility of following microstructure evolution and IASCC susceptibility of a single heat of material. It would generate the ideal material for supporting validation of cracking models, evolution of microstructure under irradiation models, and hypotheses generated from the study of plant materials. The material and data would be available to any United States' university or research laboratory. Furthermore, success in the establishment of such a program would allow building the foundation to generate materials

at higher fluence in the future. Alternative irradiation techniques may be appealing, but there currently is no guarantee that they will allow successful prediction of plant material behavior and one may not want to wait another 10 years to start an irradiation program needed to generate 100-dpa materials.

As generation of new materials for high-fluence IASCC studies is tied to either very long neutron irradiation program and/or uncertainties in the representativeness of the materials generated, one may want to study the potential influence of various microstructure features to IASCC using available material. Several programs aiming for single variable experiments are suggested. Those programs are presented in a way as to be executed with material available at the time of the writing of this report.

2.2.1 Irradiation Program: Spectrum and Flux Effect for a Re-Irradiation Program

2.2.1.1 Background and Test Plan. In order to access to the very high-fluence materials needed for this study, using research reactors to add fluence to existing irradiated materials is often considered. Some harvested components (e.g., Zorita) received up to 50 dpa and adding 20 dpa in a research reactor to reach 70 dpa appears to be a fast and economical way to obtain 70-dpa materials. However, the consequences of using a reactor with a different spectrum and flux must be considered.

The change of spectrum will influence the transmutation rate and generation of species (such as helium and hydrogen) that are suspected to play a role in the evolution of the microstructure at higher doses. Therefore, the resulting microstructure would be different. An irradiated microstructure is also a result of the competition between generation of irradiation-induced defects and thermal recombination. Such a balance can be maintained with different fluxes when fresh material is used for an irradiation campaign by adjusting the temperature. For instance, the irradiation performed at BOR-60 to emulate a 288°C irradiation in a BWR was performed at 320°C. However, it can be difficult to use this approach when an existing irradiated microstructure is already present. Some features may be annealed by the higher irradiation temperature and there is little to no data about the stability of the irradiation-induced precipitates that are expected at high fluence. In summary, it appears that irradiating a pre-existing microstructure is likely to lead to a final microstructure that is not representative of the microstructure of a LWR component. It is understood that any irradiation-induced microstructure is dependent on the operational history of the reactor and the component's location; however, there is no guarantee that the microstructure resulting from such re-irradiation would be representative of any of these conditions. Furthermore, any flux effect may not have the same consequences on microstructure with various levels of initial accumulated fluence. The behavior of the resulting microstructure with regard to IASCC susceptibility would likely be of interest for the study of IASCC, but it would probably not be wise to use such results to manage commercial reactors. Because there are still uncertainties about the role of some features, the difference induced by such irradiation may not completely prevent the acquisition of relevant data. For instance, it was not demonstrated that swelling has an impact on the intrinsic susceptibility of a material to IASCC. Therefore, an irradiation condition that would mainly lead to a different swelling content in a material would not negatively impact a program whose goals would be to determine CGR. Considering the cost associated with such re-irradiation and the advantage of utilizing re-irradiation, it is recommended that a preliminary study be performed to address the effect of flux and spectrum on the irradiation of a pre-existing microstructure.

Investigating the validity of using a test reactor to add fluence to a material that was previously irradiated in a PWR is proposed (i.e. to demonstrate that the final microstructure corresponds to what would have been obtained in a PWR). Ideally, this study would start with the use of specimens from a single material irradiated in the exact same conditions in a PWR, but with different accumulated fluence. Because this material is not available, the use of a series of thimble tubes material with different accumulated fluences will be used. The selected areas of tubes to be studied were located at the same axial elevation respective to the active fuel and are expected to have experienced the same average temperature ±10°C. The flux is similar and the difference in accumulated fluence is due to the exposure

time of the component. All tubes are made of 15%CW 316 and meet the chemical composition specification of 316 type stainless steel. However, they are from different heats and the compositions are not identical. The irradiation temperature is known.

To verify that it is possible to emulate PWR irradiation conditions using a research reactor, two sets of specimens will be used. Each set contains one piece of each of the three thimble tubes. Set number 1 contains a 19-dpa material for Tube A, a 31-dpa material for Tube B, and a 55-dpa material for Tube C. The 19-dpa material will receive an additional 12 dpa in a research reactor to reach 31 dpa, and its microstructure will be compared to the microstructure of the 31-dpa material from the harvested component. The 31-dpa material will receive an additional 24 dpa in a research reactor to reach 55 dpa, and its microstructure will be compared to the microstructure of the 55-dpa material from the harvested component. A similar approach will be performed with a second set of specimens containing 31-dpa material, a 51-dpa material, and a 74-dpa material. The research reactors that will be used are ATR and the High-Flux Isotope Reactor (HFIR), which would provide a fast flux of 10^{14} n/cm^2-s and $2x10^{15}$ n/cm^2-s, respectively. In those reactors, two irradiation conditions will be used: (1) the initial irradiation temperature (i.e., temperature experienced in a PWR) and (2) the temperature calculated to address the increased flux for each reactor.

For each irradiation path, the material will be characterized for dislocation loops, voids, bubble, and precipitation.

2.2.1.2 Outcome. This irradiation and characterization will provide a comparison between microstructures obtained in a PWR and the microstructures obtained after irradiation of a pre-existing microstructure in two research reactors with higher flux and mixed spectrum. A conservative prediction of the dose accumulated over the years in the lowest flux reactor is presented in Table 1. After approximately 2 years, initial data should provide indication about the relevance of using HFIR as a research reactor to further irradiate harvested components. HFIR is unlikely to be a candidate for irradiating the biggest IASCC test specimens needed (i.e., compact tension [CT] specimens) because of its limited irradiation space. However, the data would support study of the flux effect and may be an indicator of the results to be expected from the ongoing irradiation performed at ATR. After approximately 5 years, initial data should provide indication about the relevance of using ATR as a research reactor for irradiated harvested components in the range of 19 to 51 dpa. At this point, it would be conceivable to plan irradiation of the existing harvested components.

Table 1. Target dose for the re-irradiation program at the Advanced Test Reactor.

Specimen	Set #1			Set #2		
Year	Dose (dpa)	Dose (dpa)	Dose (dpa)	Dose (dpa)	Dose (dpa)	Dose (dpa)
0	**51**	31	19	**74**	51	31
1		33.5	21.5		53.5	33.5
2		36	24		56	36
3		38.5	26.5		58.5	38.5
4		41	29		61	41
5		43.5	31.5		63.5	**43.5**
6		46	**34**		66	46
7		48.5			68.5	48.5
8		**51**			71	**51**
9					**73.5**	

2.2.1.3 Additional Irradiation Condition. Performing the same experiment in reactors offering higher flux or larger irradiation capacity is recommended. No such reactors are available in United States; however, collaborations with international partners or with existent DOE program (i.e., IRP NEUP) may offer the capability to perform such irradiation in BOR-60 (Russia), SM-3 (Russia), or HANARO (South Korea).

2.2.2 Long-Term Irradiation for Generation of a Continuous Set of Irradiated Material

The purpose of this irradiation program is to generate high-fluence materials that will be used to study the evolution of material microstructure within a large range of accumulated fluence up to high fluence and its influence on IASCC. The interest of this approach is to follow progression of the microstructure (and IASCC susceptibility) of the same heat of material under stable irradiation conditions; therefore, circumventing the issues faced while using data from harvested components (i.e., various heats of materials and different irradiation history). As such, there is a need for irradiating several heats of material from 0 to 60 dpa.

As discussed previously, the ATR center flux trap is used to plan this activity. This position has been chosen to host this irradiation plan because of its spectrum, presence of a water loop that would be beneficial for temperature control, and its potential for a flexible test irradiation train that would facilitate maintaining such a long irradiation program by facilitating the sharing of the position used for this program. This reactor has the potential to irradiate a set of specimens from PWR spectrum and flux to a flux about a magnitude higher. However, the flux currently available leads to very long irradiations and the feasibility of this program is debatable. The irradiation program only presents the conditions for generating specimens up to 60 dpa. To achieve higher dose (i.e., up to 100 dpa) the irradiation would need to be continued or some material that experiences high fluence in service will be used to receive additional dose. This re-irradiation program and its potential limitations were discussed previously in Section 2.2.1.

2.2.2.1 Material and Specimen Selection. The materials selected are materials found in baffle and baffle bolts in various PWR concepts: SA316, with cold work level up to 15%, SA304, and SA 347. These materials correspond to the baffles and baffle bolts and thimble flux tubes. The irradiation program will create the specimens needed to generate the required data (e.g., CGR, crack initiation, and microstructure), which translate to CT specimens sized to be tested in relevant K, tensile specimens for mechanical properties characterization, specimens designed for crack initiation studies, and material for microstructure characterization.

Complete traceability of the material will be required. The material will be procured in enough quantity to have sufficient archive material to support other future irradiation programs.

2.2.2.2 Irradiation and Test Plan. The irradiation plan suggests use of the positions located at the flux trap to benefit the maximum flux available. The irradiation temperature target is 320°C, although the role of gamma heating across the specimen must be considered. The full 80 cm of the core of the ATR center flux trap is considered for use. The specimens will be loaded in capsules about 20-cm long, with four sets of capsules fitting in the core. Each capsule will host two CT specimens of each material, four flat tensile specimens of each material, and 3-mm diameter discs with a thickness of about 0.2 mm (transmission electron microscope [TEM] discs) for each material.

The irradiation would provide the following:

- 6 CT specimens, 5 tensile specimens, and TEM discs at the each of the following doses: 15 dpa, 30 dpa, 45 dpa, and 60 dpa.
- 6 CT specimens, 5 tensile specimens, and TEM discs at 60 dpa to be further irradiated.

For each dose, each material will be characterized using TEM for dislocation structure and vacancies characterization and CGR will be determined and flat specimen available for initiation.

Table 2 presents the estimated accumulated doses in each capsule as a function of time. The time at which the capsule is removed from the reactor in indicated.

Table 2. Dose rate as a function of time for each capsule. The darker area represents the capsule to be removed from the reactor.

Year	Dose Capsule A (dpa)	Dose Capsule B (dpa)	Dose Capsule C (dpa)	Dose Capsule D (dpa)
0	0	0	0	0
1	3	3	3	3
2	6	6	6	6
3	9	9	9	9
4	12	12	12	12
5	15	15	15	15
6	18	3	18	18
7	21	6	21	21
8	24	9	24	24
9	27	12	27	27
10	30	15	30	30
11	33	18	3	33
12	36	21	6	36
13	39	24	9	39
14	42	27	12	42
15	45	30	15	45
16	48	33	18	48
17	51	36	21	51
18	54	39	24	54
19	57	42	27	57
20	60	45	30	60

2.2.2.3 Outcome. This program will provide the following for several single heats of material irradiated at stable temperature and flux:

- Characterization of the evolution of the microstructure as a function of accumulated fluence
- Characterization of the evolution of the IASCC CGR as a function of accumulated fluence
- Specimens available to study IASCC initiation susceptibility.

It is well understood that this program is very long and represents a significant investment in the future. The IASCC community cannot rely solely on such irradiation given the timeline associated with it in the current available conditions. However, generation of a controlled set of specimens that are irradiated at a known and controlled temperature and dose rate would not only prove valuable to validate available data generated with other reactors, the theory, the models, and the assumptions being developed, but it will also provide a set of material that is available to receive further dose when the need arises.

2.2.3 Effect of Hydrogen in Irradiation-Assisted Stress Corrosion Cracking Susceptibility

2.2.3.1 Background. Under PWR conditions, an extensive production of helium and hydrogen will occur. It was shown (Garner et al. 2006) that these produced gases can be stored in the irradiated microstructure (i.e., dislocation, voids, and bubbles). Connerman et al. and Greenwood et al. (Connerman et al. 2005, Greenwood et al. 2004) both found evidence of such phenomena in 316CW stainless steel irradiated up to 70 dpa. Work from Edwards et al. (2009) also suggests that gas-filled cavities may be present at a dose as low as 30 dpa. Hydrogen is present in the material due to neutron-induced transmutation; therefore, its concentration is fluence-dependent. However, most of the hydrogen is present in the material due to environmental processes; therefore, it is dependent on exposure to the environment. In the case of unirradiated components, an important role of hydrogen in stress corrosion cracking in a PWR is often dismissed because of the high temperature of the material and the hydrogen's high mobility. However, considering highly irradiated materials, a significant amount of hydrogen well in excess of that predicted by Sievert's law can remained trapped in the material. Edwards et al. (2003) reported up to 3,710 appm of hydrogen in the Tihange baffle bolt 2K1R5. The efficiency of trapping depends on the irradiated microstructure (e.g., voids, bubbles, dislocations, martensitic phase created by strain, etc.).

Hydrogen in the material can influence cracking in several ways. Hydrogen is known to significantly influence dislocation behavior, increasing localized deformation and playing a role in cracking (Chateau et al. 2002a, 2002b; Magnin 2001; Girardin and Delafosse 2004). The potential role of hydrogen could increase CGR, but it also could increase crack initiation susceptibility at PWR temperature. Hydrogen embrittlement occurs in stainless steels when the material is hardened (due to the presence of martensite, precipitation, or cold work) to a hardness exceeding 310 to 350 HV. Those conditions will be met by highly irradiated materials. At low temperatures (i.e., below 100°C), hydrogen is also known to embrittle austenitic steels, particularly when martensitic transformation occurs during plastic deformation. This effect could be enhanced by development of local ferrite around bubbles due to radiation-induced segregation at very high doses. An increased embrittlement would lead to crack initiation during power outage, with this crack being the initiation site for IASCC.

In order to determine the effect of an increase of hydrogen in the material on the material susceptibility to IASCC, it is suggested to use irradiated materials and vary the amount of hydrogen trapped in the material. The materials generated will be used to study the consequences on crack initiation and propagation at temperature, but also the consequences of crack initiation at low temperature.

2.2.3.2 Test Plan and Outcome. One of the materials of interest is a thin thimble tube material that was characterized by Edwards et al. (2003). Other materials of interest are the 304 and 316 Hex block materials that were irradiated in Experimental Breeder Reactor-II. Although the irradiation conditions will not permit direct use of the data for light water reactor application, the material only has limited amount of helium trapped (i.e., less than 10 appm) and a negligible amount of hydrogen, but it also has a lot of defects (such as voids) that will store hydrogen. Therefore, it is possible to vary the hydrogen content within the material and study its effect on cracking. For thin specimens, hydrogen can be charged cathodically. One of the advantages of the Experimental Breeder Reactor-II materials is that their high-irradiation temperature (i.e., the maximum time-averaged temperature inside the highest dose block is estimated to be 460°C) would allow the use of thermal hydrogenation and potentially the use of thicker specimens. Thermal hydrogenation is an efficient method for increasing hydrogen concentration in bulk on a material that requires exposing the material to high-pressure hydrogen (i.e., greater than 1,500 psi) at elevated temperature for extended period of time (Girardin and Delafosse 2004). Maintaining temperature permits a uniform distribution of hydrogen through the thickness of the specimen. The use of this technique will require post-irradiation annealing experiments as described by Busby et al. (2002) to ensure that not irradiation-induced defects are being annealed in the process. After hydrogen loading, a desorption technique will be use to estimate the amount of hydrogen introduced into the material.

Prior to hydrogen loading, the microstructure of the material will be characterized for irradiation-induced defects, residual cold work, and ferrite content. At high dose, radiation-enhanced martensite formation during deformation was observed in austenitic 304 and 316 stainless steels (Gussev 2009a, 2009b). This phenomenon will be replicated on a set of specimens.

Flat constant extension rate tensile specimens, with doses of 20, 30, 50, and 70 dpa, will be used for this study. After hydrogen charging (up to 2,400 appm), interrupted constant extension rate tensile experiments and constant load experiments in a PWR environment at 320°C will determine the strain and stress at crack initiation time and the time to initiation at a given stress as a function of hydrogen concentration. The effect of hydrogen content in cracking at room temperature will also be characterized.

2.2.4 Effect of Strain Localization in Irradiation-Assisted Stress Corrosion Cracking Initiation

2.2.4.1 Background. Under irradiation, the microstructure's modification leads to strain localization due to the evolution of the dislocation structure and vacancies. The observed hardening of the material is partially due to the accumulation of dislocation loops. When the material begins to deform, the first dislocations sweep away those obstacles leading to strain localization associated with the apparition of dislocation channels (Byun 2006). Those two phenomena may lead to heterogeneities in deformation of the material due to dose accumulation. At high fluence, irradiation induced precipitation may generate hard obstacles that would introduce long-range stress hardening by Orowan mechanism and decrease the tendency to form channels. Additional changes in local composition (such as those due to radiation-induced segregation) will also disturb the chemical homogeneity along grain boundaries and, under very high fluence, along bubbles. Irradiation-induced grain hardening may lead to local strain due to deformation such as grain boundary sliding.

When a component is unloaded and reloaded differently (e.g., the baffle bolts may be during their lifetime), then structure instability occurs. The dislocation structure is destabilized by a change in strain path. The re-arrangement of the dislocation structure will lead to local heterogeneities that were shown to be deleterious to stress corrosion cracking. It is plausible that this effect would lead to crack initiation when components are reloaded due to swelling. Finally, fatigue is known to generate local deformation in persistent slip bands. The bands are formed due to a low reversibility of the dislocation behavior. With highly irradiated materials and significant hardening due, in part, to the presence of voids, bubbles, and precipitates, it is likely that fatigue will lead to locally enhanced plasticity.

In summary, highly irradiated materials have many opportunities to be subject to strain localization and strain localization is suspected to be an important factor in crack initiation and, potentially, crack propagation. Therefore, it is recommended that the level of strain localization due to grain boundary sliding, fatigue, and complex strain paths as a function of dose is quantified and the influence of such local deformation in the material susceptibility to IASCC is also quantified.

2.2.4.2 Test Plan and Outcome. The quantification of strain localization and the effect of strain localization of IASCC will be determined on types 304 and 316 stainless steels. The material for this study will be material irradiated at Experimental Breeder Reactor-II up to 33 dpa; baffle bolt materials and 304 and 316 plates will be irradiated at BWR temperature. Focus will be on grain boundary sliding, persistent slip bands (i.e., fatigue instabilities), and structure instabilities due to a complex strain path. The Hex block material and baffle bolts material will allow generation of local instability characterization, but will also quantify the influence of such instability on CGR and initiation. Plates of 304 and 316 will be used because this issue is also a potential concern for BWRs. The methodology for such activity was developed by Couvant (2004, 2009, 2011, 2014) and will be used for this study.

- Effect of grain boundary sliding on the time to initiation:

  Using constant extension rate tensile specimens deformed at low strain (less than 1%) with a deposited grid, grain boundary sliding and local deformation will be characterized. The specimens

will then be exposed to the environment and deformed at several constant strain rates. Using interrupted tests, the contribution of grain boundary sliding and local deformation grain boundary sliding to stress corrosion cracking initiation will be quantified as a function of grain boundary misorientation.

- Effect of fatigue on the time to initiation:

  Development of fatigue microstructure and development of localized deformations and its consequences for IASCC initiation will be investigated. Specimens with blunted notches will be submitted for fatigue loading at 290°C and 340°C for various loading rates, R (ratio between maximum stress and minimum stress), and mean stresses. The specimen will be exposed to the environment. For each condition, the degree of localization (density of persistent slip bands) and time to initiation will be generated

- Effect of substructure instabilities on the time to initiation:

  The material issue of the baffle bolt will be loaded such as different strain paths are applied and time to initiation will be determined as a function of the strain path. The same approach will be applied with other materials (e.g., materials that were not previously pre-strained in service), although less restriction will apply to generation of a different strain path. The specimens will be tested using constant extension rate tensile and constant load test. The minimum strain and/or time to initiation will be determined as a function of strain path for several doses.

2.2.5 Effect of Swelling on Irradiation-Assisted Stress Corrosion Cracking Propagation

It is well known that swelling will occur in highly irradiated materials at temperatures relevant to PWRs. This phenomenon is usually expected to play a role in loading of the components. The subject to be addressed in the context of high-fluence IASCC is the influence of a voided microstructure on crack propagation. For crack propagation, one can expect a high density of voids (both inter granular and intragranular) to affect the propagation of a stress corrosion cracking crack. Intragranular void may affect local stress and deformation and the presence of intergranular bubbles may affect grain boundary cohesion and any diffusion process on the grain boundary. Investigating the influence of void swelling on IASCC propagation is proposed.

2.2.5.1 Test Plan and Outcome. Use 304 stainless steel material irradiated in Experimental Breeder Reactor-II to study the potential effect of swelling on CGR is proposed. Because of gamma heating, the materials offer a range of void swelling and helium concentrations, while other parameters (e.g., material composition and flux) were similar. For these reasons, it is a good candidate material for performing a parametric study on the effect of void swelling on crack propagation. A schematic of a section of this material (i.e., one Hex Block) is presented Figure 1.

The 0.25 specimens will be cut such that the IASCC crack will grow in an area with a specific swelling content. In the example presented in Figure 1, two specimens will be cut so the cracks grow in the 4% swelling area and two will be cut so the cracks grow in the 2% swelling areas. From each blank of the CT specimens, a thin plate will be cut out parallel to the specimen. The CT specimens will be tested in a 320°C PWR environment. CGR will be determined at K = 10 and 18 ksi$\sqrt{in}$. TEM specimens will be machined from the thin plates such that the microstructure of the material along the crack path of the adjacent CT specimen will be determined. Fracture toughness will be determined at the end of the experiments.

This activity will determine the role of swelling on IASCC CGR.

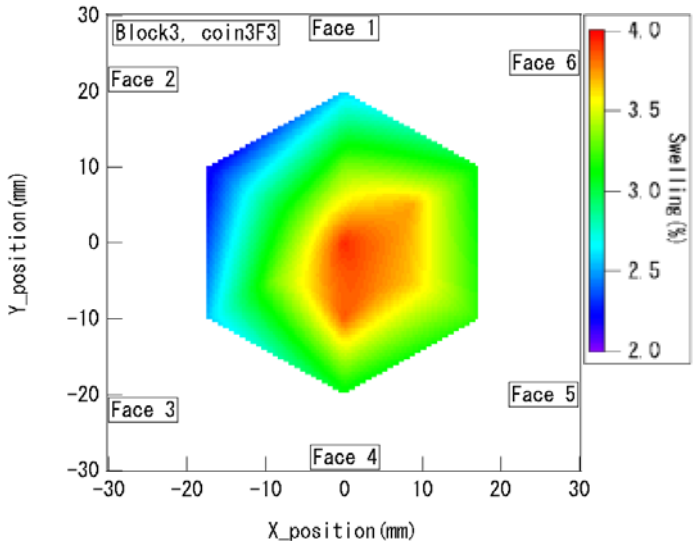

Figure 1. Ultrasonic image of the center of a Hex block of alloy 304 showing the swelling gradient across the block.

3. HIGH FLUENCE IRRADIATION-ASSISTED STRESS CORROSION CRACKING FOR BOILING WATER REACTOR MATERIALS

3.1 Introduction

As nuclear power plants age, it is necessary to determine if there are any changes in the behavior of the material as fluence increases and if the current disposition curves are sufficient to permit safe life extension of the reactors. In order to determine the remaining service life of the components, it is necessary to know the CGR of an existing flaw and to evaluate the allowable flaw size as fluence increases. For BWRs, locations such as the core shroud experience 0.5 to 1 × 10^{20} n/cm^2 (about 0.14 dpa) per effective full power year at a flux around 2 × 10^{13} n/cm^2-sec. This gives an accumulated fluence of 3 to 6 × 10^{21} n/cm^2 (4 to 8.4 dpa) after 60 years of service and up to 4 to 8 × 10^{21} n/cm^2 (5.6 to 11.2 dpa) after 80 years of service (Pathania et al. 2009). The few CGR data available at high fluence (i.e., greater than 3 × 10^{21} n/cm^2 or 4 dpa) suggest that the efficiency of the hydrogen water chemistry (HWC) mitigation technique decreases for the high stress intensity factor (K) applied. Although stress relaxation may sufficiently decrease K in service to minimize such an effect, there is concern that the disposition curve generated for lower fluence may not be conservative for high-fluence material. Moreover, a transition in the response of the material to IASCC as a function of fluence suggests either a fundamental change in the cracking mechanisms involved or underlines the fact that the role of some local phenomena, peripheral with low dose material, becomes important as fluence increases. Therefore, it appears that confirming a change in the IASCC CGR response of a material as a function of K applied for increasing fluence level is not only valuable to ensure safe operation of aging power plants, but it may be an opportunity to deepen our understanding of an IASCC mechanism that could have impact beyond the BWR community.

3.1.1 Background

3.1.1.1 Review of Crack Growth Rate Data. HWC has been well established as an efficient mitigation technique for stress corrosion cracking with unirradiated materials. CGR obtained in HWC can be 5 to 50 times lower than those obtained in normal water chemistry (NWC) (Andresen et al. 2002, Andresen and Morra 2008). Figure 2 shows the crack growth response when switching from an oxidizing environment (i.e., NWC) to a low potential environment (i.e., HWC) for a 316L stainless steel (20% cold

work). In this case, the benefit of HWC is a decrease of CGR by 14. In the NRC-NUREG-0313 report (Hazelton and Koo 1988), the disposition curve for CGR as a function of K for unirradiated material is expressed as

$$\frac{da}{dt} = A \times K^{2.161} \quad (1)$$

where K is in Mpa√m and da/dt in m/s. With A = 2.1 × 10-13 in water containing 8 ppm DO and A = 7.0 × 10-14 in water with 0.2 ppm DO, which would correspond to low potential environment. In those curves (Figure 3), the HWC mitigation efficiency is credited with a factor of 3.

As a material accumulates dose, its susceptibility to stress corrosion cracking increases and cracking is said to occur by IASCC. CGR increases rapidly with dose and, compared to unirradiated stainless steels, it is common to find CGR elevated by a factor 5 or more for K greater than 10 MPa√m. EPRI proposed a CGR versus K disposition curve based on CGR data generated with material at fluence below 3×10^{21} n/cm^2 tested in BWR water chemistry conditions (Pathania et al. 2009). It is expressed as

$$\frac{da}{dt} = B \times K^{2.5} \quad (2)$$

where K is in Mpa√m and da/dt in m/s. B = 4.564 × 10-13 in NWC and B = 1.51 × 10-13 in HWC.

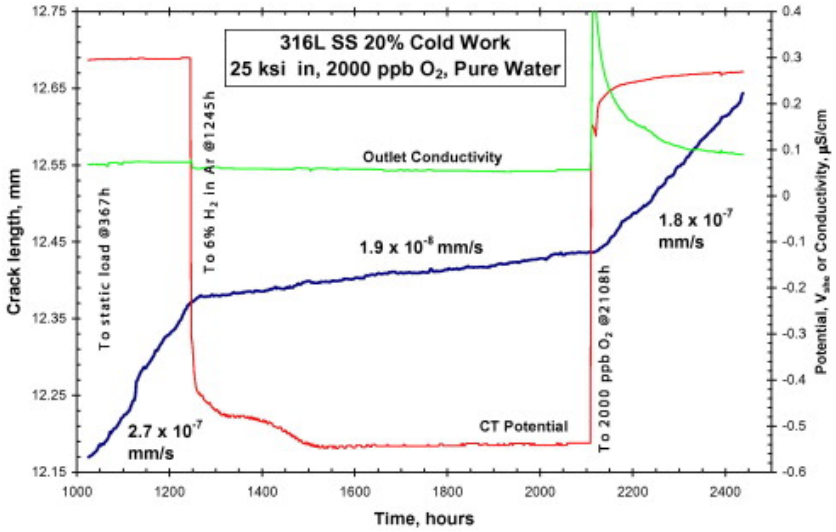

Figure 2. Effect of corrosion potential on the crack growth rate response of unsensitized 316 L, 20%Cold worked (from Andresen and Morra 2008).

When looking into the behavior of stainless steels irradiated above 3×10^{21} n/cm^2, data suggest that the expected decrease in CGR when applying HWC may disappear as dose increases. Jensen et al. (2003) tested a control blade material that was in operation for about 23 years. The material accumulated about 12 dpa and was tested to a K up to 18 Mpa√m. They observed a high CGR in HWC and concluded that under such testing conditions, HWC did not mitigate IASCC. However, while testing a 304L core shroud material irradiated in the BOR-60 fast reactor at 5.5 and 10.2 dpa, Jensen et al. (2003) did observe lower CGR when testing at low corrosion potential; however, they did not see any K dependency between K = 11 Mpa√m and K = 18 Mpa√m (Jensen et al. 2009). Takakura et al. (2009) measured CGR for 316L and 304L tested in a BWR environment. They looked at the effect of electrochemical corrosion potential as fluence increases on CGR. Their findings suggest that the effect of electrochemical corrosion potential on CGR becomes weak when the K that is applied is greater than 20 Mpa√m. Horn et al. (2013) demonstrated that HWC did not decrease CGR when testing 316NG at 3 and 4 dpa under K greater than 18.7 ksi√in, although there was a noticeable decrease in CGR when a 4.6 dpa 316NG was tested at K = 15.5 ksi√in. The IASCC growth rate of various grades of stainless steels materials tested in HWC and

irradiated in BWR conditions are plotted in Figure 4, along with the EPRI disposition curve for irradiated stainless steels in HWC. For K value greater than 15 ksi√in (16.5 MPa√m), the CGR obtained are significantly above the disposition curves.

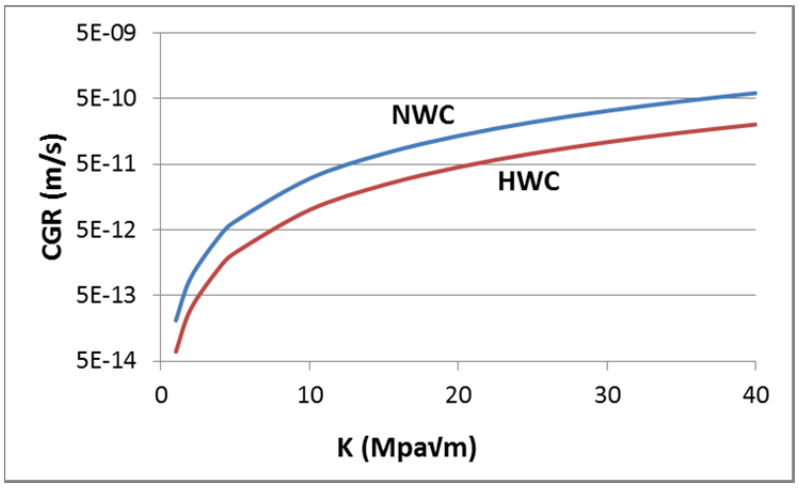

Figure 3. The NUREG-0313 disposition curve for stainless steels in normal water chemistry and hydrogen water chemistry.

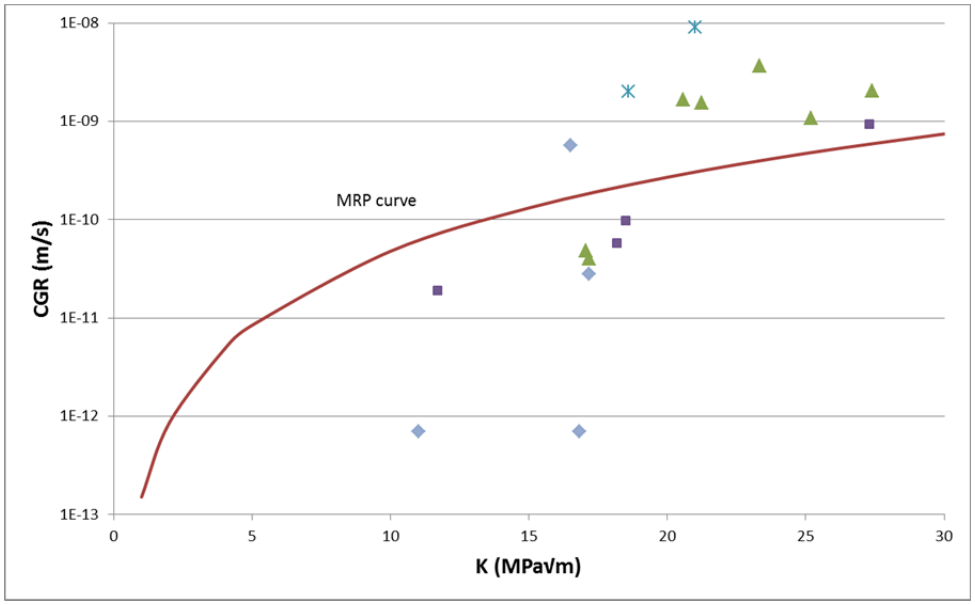

Figure 4. Crack growth rates as a function of stress intensity factor applied for doses greater than 3 dpa plotted against the Electric Power Research Institute disposition curve. The data used in this graph were extracted from (Jensen et al. 2003, Takakura et al. 2009, and Horn et al. 2013).

It is often mentioned that as fluence is accumulated in the material radiation-induced stress relaxation occurs. As stress relaxes, the K experienced by the component will decrease; therefore, high K may never be experienced by the component. Although stress relaxation occurs, it is nevertheless necessary to determine the evolution of CGR as fluence and K increases. Practically, these data can be used in correlation with stress relaxation data and weld residual stress prediction.

3.1.1.2 Effect of Specimen Size on Stress Intensity Factor Validity and Irradiation Conditions.

The specimen size and mechanical properties determine the allowable K for each CGR testing. To prevent issues that would lead to invalid CGR data, the specimen should be designed to allow maintenance of K-size validity, while permitting application of the range of K selected and the provision of sufficient material for crack advance during the various test segments. The stress intensity validity of a specimen is determined by the American Society of Testing and Materials (ASTM) E399 criteria (designed for plane strain fracture toughness testing) or ASTM E647 (designed for fatigue crack growth testing), which is less stringent. ASTM E399 is considered more appropriate for testing stress corrosion cracking. This standard provides the relationships between the geometry of the specimen and the mechanical properties of the material to determine the allowable K. The standard has been developed for material that exhibits work hardening. However, for irradiated materials that exhibit high yield stress (YS) due to radiation hardening and strain softening, the standard is not conservative. For irradiated materials, using an effective YS to determine K validity was proposed (Andresen 2011). The effective YS is defined as

$$YS_{eff} = \frac{YS_{irrad} - YS_{unirrad}}{\alpha} + YS_{unirrad} \quad (3)$$

where YSirrad is the irradiated YS at temperature, YSunirrad is the unirradiated YS at temperature, and α is a discounting factor equal to 2 or 3 (based on experience).

YSeff is used in the following equations to determine the maximum K allowable at the beginning of the test and crack advance:

$$B_{eff} \geq 2.5 \left(\frac{K}{YS_{eff}}\right)^2 \quad (4)$$

$$W - a \geq 2.5 \left(\frac{K}{YS_{eff}}\right)^2 \quad (5)$$

where W is the width of the specimen, the crack length, and Beff the effective thickness as defined in Figure 4.

As fluence increases, irradiation hardening occurs, leading to an increase of YS. Figure 5 presents an estimation of the evolution of YS for 304 stainless steel and 316 stainless steel. These correlations have been developed by EPRI (Demma 2010). The YSirrad predicted by these correlations has been used to calculate allowable K for several specimen geometries considered in this program. The results are summarized in Tables 3 and 4. When the allowable K decreases significantly as cracks grow (a/w increase), the values at several a/w are given. Five CT specimen designs are considered: (1) standard 0.4 T-CT with normal thickness, (2) 0.4 T-CT with reduced thickness, (3) 0.5 T-CT with normal thickness, (4) 0.5 T-CT with reduced thickness, and (5) 0.6 T-CT with reduced length.

It should be noted that the Nakamura et al. (2007) and Sumiya et al. (2007) analyses suggest that a stable, valid, CGR can be obtained even after K exceeds the upper limit determined with the effective stress concept. It also is accepted that the best determination of the validity of a CGR test is based on the cracking behavior recorded. However, considering that this report suggests the machining of specimens prior to irradiation, it is recommended to have a conservative approach when designing specimen.

In addition to influencing the maximum allowable K, specimen thickness also affects the temperature gradient across the specimen during irradiation. Figure 6 presents the temperature gradient obtained when a stainless steel 0.5 T-CT is being irradiated in ATR's pressurized water loop and receiving 1.58×10^{14} n/cm^2-s (the highest flux considered in this report). The temperature difference between the specimen surface and the center of the specimen is 55°C (Tyler et al. 2014). The temperature difference dropped to 35°C for a 0.4 T-CT specimen and is below 20°C for a specimen with a thickness equal at 0.3 in. Therefore, using the thin specimen is encouraged when possible. Thin specimens also are advantageous because more can be irradiated in a test capsule.

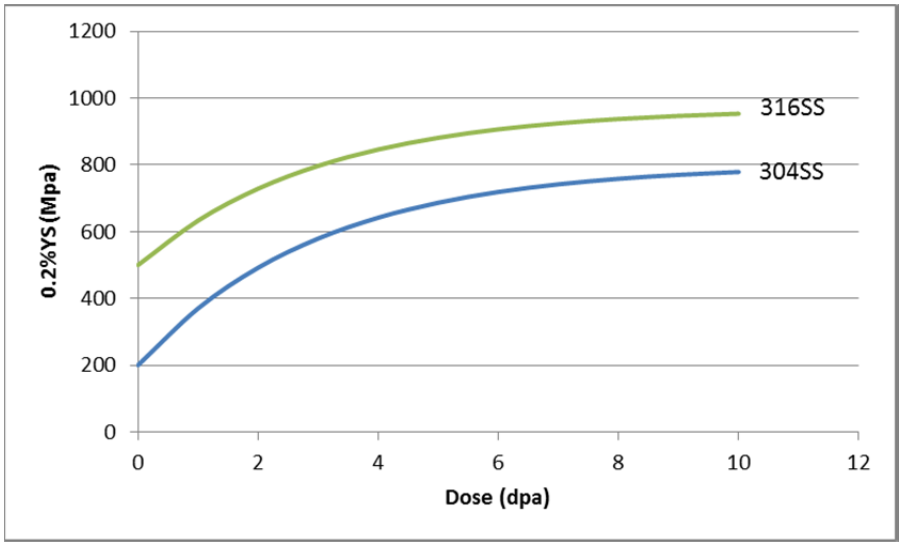

Figure 5. Yield strength as a function of dose for stainless steels at 270 to 330°C (according to Demma 2010).

Table 3. Prediction of allowable stress intensity factor (ksi√ in) for the specimen geometries considered for 304 stainless steel.

Specimen Description	B_{eff}	W	2 dpa	4 dpa	8 dpa
Estimated Irradiated YS			491 Mpa	641 Mpa	758 Mpa
0.4 T-CT	0.38	0.8	K_{max} = 18.4	K_{max} = 22.6	K_{max} = 25.9
			K_{max} (a/w:0.58) =17.35	K_{max} (a/w:0.58) =21.3	K_{max} (a/w:0.58) =24.4
					K_{max} (a/w:0.65) =22.3
	0.28	0.8	K_{max} = 15.8	K_{max} = 19.4	K_{max} = 22.3
0.5 T-CT-1	0.47	1	K_{max} = 20.4	K_{max} = 25.2	K_{max} = 28.8
			K_{max} (a/w:0.58) =19.3	K_{max} (a/w:0.58) =23.8	K_{max} (a/w:0.58) =27.3
			K_{max} (a/w:0.65) =17.6	K_{max} (a/w:0.65) =21.7	K_{max} (a/w:0.65) = 24.9
	0.28	1	K_{max} = 15.8	K_{max} = 19.4	K_{max} = 22.3
0.6 T-CT	0.57	1.2	K_{max} = 22.5	K_{max} = 27.7	K_{max} = 31.8
				K_{max} (a/w:0.58) = 26.1	K_{max} (a/w:0.58) =29.9
			K_{max} (a/w:0.58) = 21.2	K_{max} (a/w:0.65) = 23.8	K_{max} (a/w:0.65) = 27.3

Table 4. Prediction of allowable stress intensity factor (ksi√ in) for the specimen geometries considered for 316 stainless steel (YS = 160 MPa).

	B_{eff}	W	2 dpa	4 dpa	8 dpa
Estimated Irradiated YS			728 Mpa	846 Mpa	937 Mpa
0.4 T-CT	0.38	0.8	K_{max} = 25.1	K_{max} = 28.4	K_{max} = 31.0
			K_{max} (a/w:0.5) =25.75	K_{max} (a/w:0.58) =26.7	K_{max} (a/w:0.58) =29.1
			K_{max} (a/w:0.58) =23.6	K_{max} (a/w:0.65) =24.4	K_{max} (a/w:0.65) =26.6

	B_{eff}	W	2 dpa	4 dpa	8 dpa
Estimated Irradiated YS			728 Mpa	846 Mpa	937 Mpa
	0.28	0.8	K_{max} = 21.5	K_{max} = 24.4	K_{max} = 26.6
				K_{max} (a/w:0.65) =24.4	K_{max} (a/w:0.65) =26.6
0.5 T-CT-1	0.47	1	K_{max} = 27.9	K_{max} = 31.6	K_{max} = 34.5
			K_{max} (a/w:0.58) =26.4	K_{max} (a/w:0.58) =29.9	K_{max} (a/w:0.58) =32.6
				K_{max} (a/w:0.65) =27.29	K_{max} (a/w:0.65) = 29.7
	0.28	0.8	K_{max} = 21.5	K_{max} = 24.4	K_{max} = 26.6

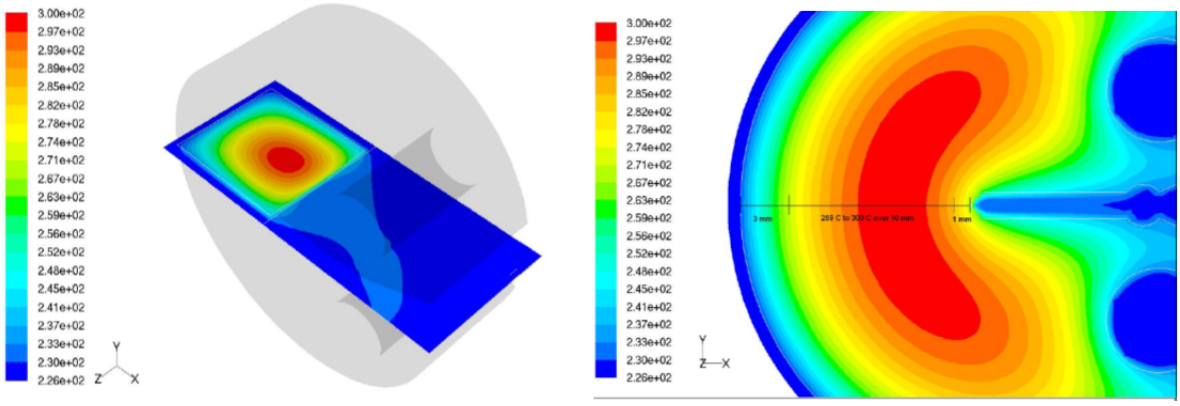

Figure 6. Temperature gradient obtained for a 0.5-CT specimen at the maximum flux considered in this report (Tyler et al. 2014).

3.1.2 Data Required

Data are needed to quantify the effectiveness of HWC mitigation on CGR for material at fluence above 3×10^{21} n/cm^2 (4 dpa) as a function of K applied. Based on the estimated fluence to be experienced by the component, operational K (discounting any relaxation effect), and previous data, it is recommended that CGR data be generated in the NWC and HWC environments under K applied, ranging from 14 to 22 ksi√in from specimens of accumulated fluence above 3×10^{21} n/cm^2 (4 dpa) and up to 7×10^{21} n/cm^2 (10 dpa). Ideally, the total fluence should be accumulated in a spectrum and flux comparable to a BWR (such as permitting direct transposition of data to components in service). However, a higher flux would be acceptable when justified by previous experiences and the known impact of flux on irradiated microstructure. The materials will need to be 300-series austenitic stainless steels (Type 304, 304L, 316L, 316NG, or 304NG), their welds, and heat affected zone (HAZ) (304HAZ and 316 HAZ). Typically, each material should be tested under several K alternatively in NWC and HWC at a given dose. Ideally, each material would be available at different dose levels.

CGR data are needed to determine the effect of fluence on the efficiency of HWC mitigation. However, it would be a mistake to only consider the short-term and immediate need for such data. The prediction of CGR and development of predictive models that will be able to predict stress corrosion cracking often requires a different set of data. This is why, in this report, a quick description of techniques used to study the fundamentals of stress corrosion cracking is proposed and why it will be suggested that, when possible, material be harvested or generated in addition to the specimen immediately needed for this program. These additional materials and specimens could be made available to the scientific community through the U.S. Department of Energy's Advanced Test Reactor's National Scientific User Facility for

future research projects. These projects would benefit a direct comparison with the CGR data to be generated by this program.

It would be beneficial to move from an empirical estimation of specimen K-size validity to a model more based on actual material mechanical response.

Fracture toughness data above 3×10^{21} n/cm^2 (4 dpa) also are desirable in order to define a transition to lower fracture toughness at fluences above 3×10^{21} n/cm^2 (4 dpa). Although fracture toughness is not the topic of this report, it will be recommended that fracture toughness testing be performed after CGR testing when possible.

3.2 Program Plans

Three program plans and their options are discussed in this report. Although they do not exclude each other, they are presented separately based on the origin of the material tested and on the equipment requirements. The facilities available to perform neutron irradiation with the specimen size required for this program and to perform IASCC experiments are limited. Therefore, several options will be presented that can be chosen from, based on the funding and equipment availability.

3.2.1 Program Plan Based on an Irradiation Program Dedicated to this Work

A dedicated irradiation and test program can be defined to generate the required CGR data. This irradiation program has the benefit of circumventing heat–to-heat variability by testing the heat of each material over the range of fluence and determined applied K. It also would permit generation of specimens, whose size will not limit testing due to a K size validity criterion.

This program proposes to generate specimens to quantify the efficiency of HWC under applied K, ranging from 14 to 22 ksi√in to doses ranging from 2 to 10 dpa. Three dose levels between 4 and 10 dpa are desirable. Data at 2 dpa would permit tying the new data to the various data available and would serve as a baseline, because HWC mitigation is expected to be efficient at such a dose under the commonly applied K. Following the irradiation program, microstructure and mechanical properties will be characterized. A CGR testing plan will be discussed.

In this report, the specimen design, cost estimate, and schedule have been determined based on the assumption that irradiation will be performed in the water loop located in the ATR center flux trap (ATR 2009).

3.2.1.1 Material Selection. The materials of interest are stainless steels and their welds. For this program, it was decided to focus on four materials to minimize the size of the irradiation matrix. Two base metals (304L and 316L) and their weld HAZ were selected. The materials will be welded under constrained conditions using shielding metal arc welding in conditions consistent with those typical of BWR core components. Complete traceability of the material will be required. The material will be procured in enough quantity to have sufficient archive material to support other future irradiation programs.

3.2.1.2 Specimen Design. T-CT Specimen – Various geometries were considered as to be able to test in the large K range considered. Based on the estimation presented in Tables 3 and 4, a program involving 316L material could be performed with 0.4 T-CT specimens for a dose of about 2 dpa and 0.4 T-CT specimens with 0.3-in. thickness can be used for higher doses. The mechanical properties predicted for irradiated 304 stainless steel call for use of 0.6 T-CT specimens for irradiation around 2 dpa; 0.4 T-CT specimens will be used for irradiation up to about 4 dpa; and 0.4 T-CT with 0.3-in. thickness will be used for specimens to be irradiated at higher doses.

The specimens made of base metal will be cut in the T-S orientation from a plate. A 5% side grove will be machined. The schematic of a 0.4 T-CT specimen is presented in Figure 7. For HAZ specimens, the CT specimens will be cut so the crack grows in the HAZ.

Tensile and TEM Specimen – Tensile and TEM specimens will be included in the irradiation for each target dose. The TEM specimens will consist of 3-mm disks. The tensile specimens will be dog bone specimens similar to the one shown in Figure 8.

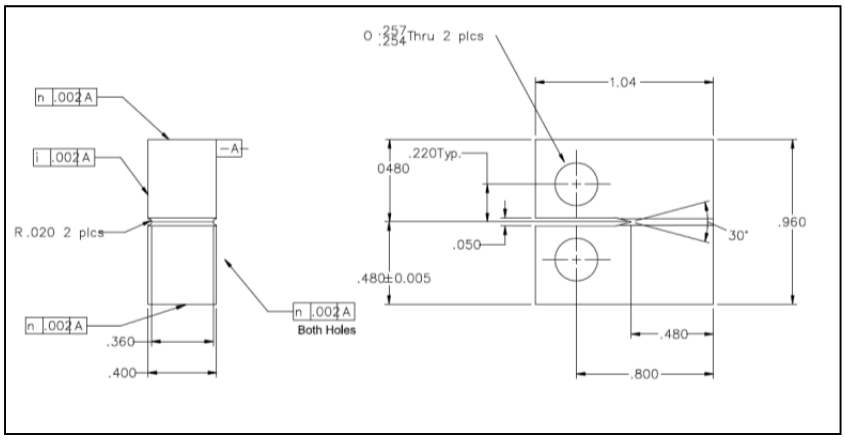

Figure 7. Schematic of the 0.4 T-CT specimen dimensions in inches.

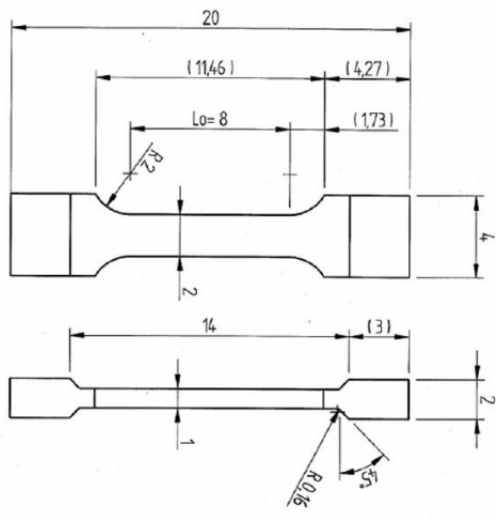

Figure 8. Schematic of a tensile specimen dimension in millimeters.

3.2.1.3 Irradiation and Test Plan. Selection of Dose Rate and Temperature – The dose rate in a BWR is about 2×10^{13}n/cm^2-sec. Under such a low flux, it would not be possible to generate specimens with the dose range required in a timely manner. Significantly increasing the dose rate experienced by the specimen raises the question of the flux's effect on the material microstructure and the CGR behavior. This flux effect has been demonstrated at low dose. However, it appears that in the region of 3 to 5 dpa, the flux effect is negligible on the factors influencing CGR (e.g., radiation-induced segregation and hardening). Therefore, it is considered to be target dose rates similar to the ones used for a similar program at the Japanese Material Test Reactor (1×10^{14} n/cm^2-s or about 2×10^{-7} dpa/s). ATR's center flux trap offers about 2×10^{-7} dpa/s (ATR 2009). An irradiation in this position would permit generation of specimens up to 10.5 dpa within 4 years. The data would be directly comparable with the data generated by the Japanese program with specimens irradiated in the Japanese Material Test Reactor. Therefore, it is proposed to perform the irradiation program at ATR. However, considering that a lower flux would be technically acceptable, other reactors can be considered, although the period of irradiation will be extended. The target irradiation temperature will be 288°C.

3.2.1.4 Test Plan and Outcome. The irradiation is designed to use about two-thirds of the more valuable real estate of ATR in order to increase the availability of the irradiation position. The target doses for the specimens are 2.5, 4.3, 7.7, and 10.3 dpa. The specimen's size will differ as a function of final dose in order to meet the K-size criteria previously determined (Tables 5 and 6). For 316-type stainless steel, the 0.4 T-CT specimen will be used for the target dose of 2.5 dpa and the 0.4 T-CT specimen with a thickness of 0.3 in. will be used for higher doses. For 304-type stainless steel, the 0.6 T-CT specimen will be used for a target dose of 2.5 dpa, the 0.4 T-CT specimen will be used for the target dose of 4.3 dpa, and the 0.4 T-CT specimen with a thickness of 0.3 in. will be used for higher doses. The test train is composed of four test capsules. Three test capsules will be located in the core of the reactor and will experience a dose rate of 1.5×10^{-2} dpa/day. A fourth capsule will be located about 9 in. from the center of the core and the dose rate will be about 0.7×10^{-2} dpa/day. The purpose of the different locations is to minimize temperature gradient through specimens of different thicknesses. Each capsule will contain CT specimens, tensile specimens, and TEM discs for one target dose. The target dose for each capsule is indicated in Table 5. Capsule D will contain four 0.6 T-CT specimens of 304L and 304HAZ. Capsule A and B, for target doses of 10.26 and 7.69 dpa, respectively, will contain thin 0.4 T-CT specimens of 304L, 304LHAZ, 316L,and 316LHAZ. Capsule C, for a target dose of 4.28 dpa, will contain 0.4 T-CT specimens of 304L and 304LHAZ and thin 0.4-T-CT specimens of 316L and 316LHAZ. When Capsule B is removed after the specimens reach 7.69 dpa, the specimens will be replaced by 0.4 T-CT specimens of 316L and 316LHAZ. This irradiation plan will generate the minimum number of specimens required in 3 years.

Table 5. Target dose for the irradiation program. The value in bold corresponds to the dose at which a capsule is removed and specimens are made available.

Capsule		A	B	C	D
Year	Cycle	Dose (dpa)	Dose (dpa)	Dose (dpa)	Dose (dpa)
1	1	0.85	0.85	0.85	0.5
	2	1.71	1.71	1.71	1
	3	2.56	2.56	2.56	1.5
	4	3.42	3.42	3.42	2
2	5	4.28	4.28	**4.28**	**2.5**
	6	5.13	5.13		
	7	5.985	5.985		
	8	6.84	6.84		
3	9	7.69	**7.69**		
	10	8.55	0.85		
	11	9.40	1.71		
	12	**10.26**	**2.56**		

After exposure, each specimen will be tested. Tensile specimens will be used to determine the mechanical properties of the material at the achieved dose. TEM discs will be used for microstructure analysis. The CGR specimens of the four heats of materials will be tested at K, ranging between 14 and 22 ksi√in (15.4 and 24.2 Mpa√m). An example of the test plan for alloy 316L is presented Table 6. The maximum target K was selected to be conservative, knowing that uncertainty in crack length measurement by dcpd may lead to an underestimation of K and sometime threaten the validity of the test. It is always the responsibility of the experimenter to estimate the validity of the CGR measured and determine if applying higher K and extending the initial K range can be done.

Table 6. Test plan for 316L specimens.

Material	316L											
Dose (dpa)	2.56			4.28			7.69			10.26		
Number of specimen	3			3			3			3		
K tested (ksi√in)	14			14			14			14		
		16			16			16			16	
	18			18			18			18		
		20			20			20			20	
			22			22			22			22
Fracture toughness			yes			yes			yes			yes
Environment per K tested	NWC and HWC											

This program will generate CGR versus K curves for four levels of fluences and quantify the effectiveness of HWC for materials experiencing up to 80 years of service.

3.2.1.5 Estimate Cost. The timeline and cost for the irradiation activity is presented in Table 7. Once the target dose is achieved for a capsule, the mechanical properties and microstructure of the materials containing a capsule can be characterized in the year following removal of this capsule from the reactor. For each material-dose couple, three CGR tests will be performed, which is about 1 year of occupancy of a CGR test loop. The plan calls for four materials and four doses, which is about 16 years of occupancy of a test loop to test all specimens and complete the test plan. A detailed timeline to complete the test plan is not provided, because it is obvious that the availability of test loops in the country for the next 16 years is not available. This project would benefit from collaboration between laboratories to obtain data in a timely manner.

Table 7. Estimated timeline and associated cost for the irradiation program.

	Activity (Irradiation Related) and Specimens Available For Testing	Estimated Cost ($K)
Year 1	Design and fabrication of test train and specimens Irradiation test plan	1,200
Year 2	Ongoing Capsule A, B, C, and D	700
Year 3	Ongoing Capsule A and B 304 materials at 2.5 dpa available All materials at 4.28 dpa available	720
Year 4	All materials at 7.69 and 10.26 dpa available 316 materials at 2.56 dpa available	740

3.2.2 Program Based on Material Harvested from Boiling Water Reactor Components

The primary objective of this program is to determine the validity of the disposition curve at fluences above 3 dpa by determining the evolution of CGR as K increases for material harvested from BWR components. The use of such material ensures that the material is fully representative of what is in the field, but it also limits the range of fluence available. However, it is possible to extend the range of fluence available with a dose accumulation program. This program is described as an additional test plan and designed based on the considerations discussed in the previous section.

3.2.2.1 Material and Specimens. Collaboration with General Electric would permit gaining access to materials removed from the cruciform region of five control rod blade handles. The materials (i.e., three heats of 316NG and two heats of 304NG) experienced up to 3.8×10^{21} n/cm^2 (5.4 dpa) in service. Mechanical characterization and microstructure analysis are available for these materials. The accumulated fluence was estimated using the power history of the reactor and was compared to retrospective dosimetry. The materials composition and accumulated fluence are presented in Table 8. The material currently is present in the United States and could be made available for this research program.

Table 8. Control rod blade material available through collaboration.

Heat ID	Material type	Dose (x 10^{21} n/cm^2)	Dose (dpa)
D802	316NG	2.8	4
D800	316NG	1.2	1.7
D790	316NG	2.1	3
D485	304NG	3.8	5.42
SND482	304NG	3.2	4.57

Because of the thickness of the source material, the specimen will be based on a standard 0.4 T-CT specimen, but with a thickness of 0.3 in. The maximum allowable K for each material type is determined using Table 4. These no-standard-specimens should offer sufficient ligaments for crack grow for the various tests segments needed for the project.

3.2.2.2 Test Plan and Outcome. Initially, testing of two heats of 316 stainless steel and two heats of 314 stainless steel is proposed. Part of this set of material had been tested previously and data have been reported by Horn et al. (2013). The data showed that HWC was effective when alloy D482 (i.e., a type 304NG stainless steel at 4.5 dpa) was tested at an applied K of 15 ksi√in (16.5 Mpa√m). HWC mitigation was not effective for two heats of Type 316NG stainless steel (i.e., D790 tested under K greater than 23 ksi√in [25.3 Mpa√m] and D790 tested under K greater than 18.7 ksi√in [20.5 Mpa√m]), although doses were slightly lower (4 dpa for D802 and 3 dpa for D790). These data need to be extended to be able to quantify the efficiency of HWC in a broader range of K applied for each heat. The heat of 304NG stainless steel (SND485), which experienced 5.4 dpa in service, will be added to this work scope. The objective will be to determine the validity of the CGR disposition curves for fluence above 2.1×10^{21} n/cm^2 (3 dpa) and below 3.8×10^{21} n/cm^2 (5.4 dpa).

The four heats of material will be tested at K ranging between 14 and 22 ksi√in (15.4 and 24.2 Mpa√m) for 316 and between 14 and 20 ksi√in (15.4 and 22 Mpa√m) for 304. These data would permit determination of the validity of the CGR disposition curve in the HWC condition at the fluence tested, determine if the current disposition curves are conservative for a given K, and provide information to determine if the industry can take credit for stress relaxation. A summary of the tests is presented in Table 9.

3.2.2.3 Estimated Timeline and Cost. Table 10 presents the estimated timeline and cost to perform the work described in this section, assuming the CGR work is performed at Idaho National Laboratory. This estimate does not consider equipment availability and assumes that one IASCC test loop will be available for this program when needed. This work represents a 6-year-long effort for a cost (excluding shipping) of about $1,300K over this period.

Table 9. Test plan for materials issued from harvested components.

Specimen ID	D802			D790			D485		D482	
Material	316NG			316NG			304NG		304NG	
Dose (dpa)	4			3			5.4		4.5	
Number of Specimen	3			3			2		2	
K Tested (ksi√in)	14			14			14		14	
		16			16			16		16
	18			18			18		18	
		20			20			20		20
			22			22				
Fracture Toughness?			yes			yes		yes		yes
Environment per K Tested	NWC and HWC									

Table 10. Estimated timeline and cost assuming that the work is performed at Idaho National Laboratory for the basic test plan.

	Activity	Outcome	Estimated Cost ($K)
Year 1	Material shipment Specimen machining	Material available for testing.	200
Year 2	Testing heats D802 and D790: two tests		280
Year 3	Testing heats D802 and D790 continued: two tests	Quantification of the efficiency of HWC mitigation for two heats of 316NG as a function of K applied (ranging from 14 to 20 ksi√in) at fluence above 3.2×10^{21} n/cm^2 (4.5 dpa).	280
Year 4	Testing heats D482 and D485: two tests		280
Year 5	Testing heats D482 and D485 continued: two tests	Quantification of the efficiency of HWC mitigation for two heats of 304NG as a function of K applied (ranging from 14 to 20 ksi√in) at fluence above 2.1×10^{21} n/cm^2 (3 dpa). Fracture toughness data.	280
Year 6	Testing heats D802 and D790 continued: two tests	Quantification of the efficiency of HWC mitigation for two heats of 316NG at K applied (about 22 ksi√in) at fluence above 3.2×10^{21} n/cm^2 (4.5 dpa). Fracture toughness.	280

3.2.2.4 Additional Irradiation Program and Test Plan. It would be desirable to establish the evolution of CGR for a given K as fluence increases. Attaining this objective will require irradiating specimens up and beyond 5 dpa. Using the heat D800 (316NG material) is proposed, which experienced 1.2×10^{21} n/cm+ (1.7 dpa), in service and to re-irradiate this material to have four accumulated fluences ranging from 1.2×10^{21} n/cm^2 (1.7 dpa) to 6×10^{21} n/cm^2 (8.5 dpa). This irradiation could be performed as a stand-alone irradiation or be part of the irradiation program described previously. The material will be tested in both NWC and HWC under five applied K, with K ranging between 14 and 22 ksi√in (15.4 and 24.2 Mpa√m). For each irradiation condition, the mechanical properties and microstructure analysis

will be performed. An estimated timetable for this activity is presented in Table 11. In accordance with the irradiation condition, this work would require three CT specimens, two tensile specimens, and TEM discs.

This additional work will provide CGR data with the same material as a function of fluence and applied K. It will provide insight about the validity of high-flux irradiation in this dose range.

Table 11. Estimated timetable for additional activity with control rod blade material.

Year	Dose Available	Activity
0	1.7	CGR at 1.7 dpa K = 14 to 20 ksi√in
1	4	CGR at 4 dpa K = 14 to 22 ksi√in
		Comparison with D802 results (4 dpa accumulated in reactor)
2	7	CGR at 7 dpa K = 14 to 22 ksi√in
3	10	CGR at 10 dpa K = 14 to 22 ksi√in

3.2.3 Program Based on Materials Generated by a Previous Irradiation Program

The objective of the primary program of this section is to determine the evolution of CGR as a function of applied K on a single heat of material for three fluence levels. Working with a single heat of material permits prevention of data scatter due to heat-to-heat variability and will clearly show the influence of fluence in the CGR behavior of the material. Moreover, the material selected represents the fusion zone of a 304L weld and few data are available for welds.

The suggested extended program is similar to the work proposed with material harvested from BWR components, where it will determine the evolution of CGR as a function of K applied at a given fluence. Additional interest resides in the testing of HAZ (304L and 316L). No HAZ was available from harvested components (and HAZ is of interest) and of HT 304L with a dose greater than 10 dpa, which corresponds to the maximum dose to be experienced by components after 80 years of life extension.

3.2.3.1 Materials and Specimens. The materials come from a Japanese national project that started in 2001. Specimens were irradiated in the Japanese Material Test Reactor in BWR conditions (e.g., temperature of 288°C [262 to 302°C] and conductivity below 0.1μS/cm [Takakura et al. 2009, Nakamura et al. 2007] at a flux of 1×10^{18} n/m^2-s). Some post-irradiation experiments (e.g., mechanical testing, microstructure characterization and CGR) have been performed and the data are available. For this project, heat-treated 304 (SUS 304HT), heat treated 316L (316LHT), and HAZ (304L and 316L) were selected. The heat treatment applied (i.e., 1030°C for 30 minutes, followed by water quench) diminished the enriched chromium (and molybdenum) concentration at grain boundaries of the as-received materials to simulate the new fusion line of the weld HAZ. The HAZ specimens were generated from the plate of 316L and 304L that were welded using shielded metal arc welding under conditions typical for most BWR core components. The D316L electrode was used to weld 316L and D308L was used to weld 304L. The specimens selected for the programs discussed in this report are presented in Table 12 (primary program) and Table 13 (extended program).

The specimens' designs are based on a standard 0.5 T-CT specimen design, but with varied thicknesses (e.g., for a specimen with less than 1.7 dpa and specimen thickness of 0.5 in. [12.7 mm] and for specimens with up to 5 dpa and specimen thickness of 0.25 in. [6.4 mm]). For specimens with higher doses, the specimen thickness is 0.22 in. (5.6 mm). The specimens were cut in the T-S orientation. Assuming an irradiation hardening similar to that discussed earlier in this report (Demma 2010), and using ASTM Standard E399 and E647 as references with a discount factor of two, specimens A105 and A106 can be tested up to K = 20.7 ksi√in (22.8 Mpa√m) and grow the crack with little constraint (a/w = 0.6 can be safely achieved). Specimens A128 and A129 can be tested up to K = 21.8 ksi√in (24.0 Mpa√m).

Table 12. Specimens available for the main program.

Specimen ID	A105	A106	A128	A129	A139	A140
Material	304HT				304LHT	
Dose (dpa)	3.82	4.49	8.6	8.9	13.6	13.4

Table 13. Specimens available for the extended program.

Specimen ID	A112	A113	A114	A102	A104
Material	304L/HAZ			304/HAZ	316L/HAZ
Dose (dpa)	3.81	3.57	3.75	3.29	3.72

3.2.3.2 Test Plan and Outcome. Four specimens made of 304HT and two made of 304LHTwill be tested successively in NWC and HWC at K = 14, 16, 18, and 20 ksi√in. The doses experienced by the selected specimens are roughly 4 dpa, 8.5 dpa, and 13.5 dpa. This range will permit demonstration of the effect of fluence on the CGR dependency to applied K. The test plan suggests testing only two K per specimen. For each K applied, two water chemistries (i.e., NWC and HWC) are to be tested. Table 14 presents the test plan suggested for this program.

Table 14. Stress intensity factor applied to HT304 specimens for the primary program.

Specimen ID	A105	A106	A128	A129	A139	A140
Dose (dpa)	3.82	4.49	8.6	8.9	13.6	13.4
K tested (ksi√in)	14		14		14	
		16		16		16
	18		18		18	
		20		20		20
Fracture toughness?		Yes		Yes		Yes
Environment per K tested	NWC and HWC					

3.2.3.3 Estimated Timeline and Cost. This program will need shipping of specimens from Japan to the United States. This estimate assumes that the work will be performed at Idaho National Laboratory and that no collaboration is established with the current owner of the specimens (located in Japan). Equipment availability is not considered. The cost and timeline associated with this activity is presented in Table 15. The work represents a 4-year-long effort for a cost (excluding specimen acquisition and shipping) of about $850K over this period.

3.2.3.4 Extended Program. The CGR of 304L HAZ, 304HAZ, and 316L HAZ at around 4 dpa will be measured at four applied K ranging from 14 to 20 ksi√in. These data will permit comparison of HAZ behavior with base metal and the applicability of the disposition curve to the welds. Table 16 presents the test plan suggested for this program. Because only one specimen is available for 304HAZ and 316L HAZ, it is expected that the results obtained with 304L HAZ will allow planning the future experiments to select the K applied accordingly. In addition, fracture toughness data will be generated, assuming satisfactory behavior of the crack.

The cost and timeline associated with this activity are presented in Table 17. This work represents a 5-year-long effort for a cost (excluding specimen acquisition and shipping) of about $1,100K over this period.

Table 15. Estimated timeline and cost for the primary program using specimen generated from a previous irradiation program.

	Activity	Outcome	Estimated Cost ($K)
Year 1	Specimen acquisition, shipment, and reception	Material available for testing in the United States.	?
Year 2	Testing specimens A128 and A129		280
Year 3	Testing specimens A105 and A106	Determination of the influence of fluence on the evolution of CGR for 304HT as a function of K. Fracture toughness data.	280
Year 4	Testing specimens A139 and A140	Determination of the influence of K applied on the evolution of CGR for 304L at fluence corresponding to the end of component lifetime. Connection, although with reserve, with 304HT data at lower dose. Fracture toughness data.	280

Table 16. Test plan for the extended program.

Specimen ID	A112	A114	A102	A104
Material	304L HAZ		304 HAZ	316L HAZ
Dose (dpa)	3.81	3.75	3.29	3.72
K Tested (ksi√in)	14		14	14
		16		
	18		18	18
		20		
Fracture Toughness?		Yes		
Environment per K Tested		NWC and HWC		

Table 17. Estimated timeline and cost associated with the extended program.

	Activity	Outcome	Estimated Cost ($K)
Year 1	Specimen acquisition, shipment, and reception	Material available for testing in the United States.	?
Year 2	Testing specimens A112 and A114	Determination of the evolution of CGR as a function of K for 304L HAZ at about 4 dpa. Fracture toughness data.	280
Year 3	Testing specimens A115 and A116	Determination of the evolution of CGR as a function of K for 316L HAZ at about 4 dpa. Fracture toughness data.	280

	Activity	Outcome	Estimated Cost ($K)
Year 4	Testing specimens A130 and A131	Determination of the evolution of CGR as a function of K for 316L HAZ at about 10 dpa. Fracture toughness data.	280
Year 5	Testing heats A127 and A138	Determination of the evolution of CGR as a function of K for 316L HAZ at about 13 dpa. Fracture toughness data.	280

4. SUMMARY

In this report, several research plans for assessing the IASCC susceptibility to high-fluence material are described. The first part of the report addresses IASCC issues for PWRs, whereas the second part addresses BWR high-fluence IASCC.

For PWRs, it was identified that there is a need for test materials irradiated in a PWR condition and a program was proposed. An alternative to a long and expensive program could be irradiation of harvested components in research reactors; however, this would require a better understanding of the effect of flux and spectrum on the irradiation of a pre-existing microstructure. A program to assess this issue was also described. As the difficulty of predicting high-fluence IASCC in PWRs is due, in part, to the lack of knowledge on the evolution of the irradiated microstructure at very high doses but also due to the lack of knowledge on the role of certain features on IASCC susceptibility, three research programs aiming to increase our understanding of the role of such features on high-fluence IASCC and the initiation of IASCC after long service are presented. They address the role of local deformation in IASCC initiation, the role of swelling in IASCC propagation, and the role of hydrogen in initiation and propagation.

For BWRs, it was identified that IASCC CGR may change under high K as dose increases. This change of behavior would decrease the mitigation efficiency of hydrogenated water chemistry. Focus was on the effort of addressing this issue because it is not only a concern for the safety of the component but because studying this change in CGR behavior has the potential to increase our understanding of the IASCC mechanism. A detailed approach of this issue, which includes an irradiation program and testing material available via collaborations with an industry partner and international partner, were described.

5. REFERENCES

Andresen, P. L., T. M. Angeliu, L. M. Young, W. R. Catlin, and R. M. Horn, 2002, *10th International Conference on Environmental Degradation of Materials in Nuclear Power Systems– Water Reactors*.

Andresen, P. L., 2004, "Factors Influencing SCC and IASCC of Stainless Steels in High Temperature Water," in proceedings of the *American Society of Mechanical Engineers - ASME, Pressure Vessels and Piping Division Conference*, July 25-29, 2004, PVP – V. 479, p 185-192.

Andresen, P. L. and M. M. Morra, 2005, "Effects of Si on SCC of Irradiated and Unirradiated Stainless Steels and Nickel Alloys," in proceedings of the *12th International Conference on Environmental Degradation of Materials in Nuclear Power Systems – Water Reactors*, TMS, p. 87.

Andresen, P. L. and M. M. Morra, 2008, *Journal of Nuclear Materials*, Vol. 383 (1-2).

Andresen, P. L., 2011, "K Size Effects on SCC in Irradiated, Cold Worked and Unirradiated Stainless Steel," *11th International Conference on Environmental Degradation of Materials in Nuclear Power Systems – Water Reactors*.

ASTM E399, "Standard Test Method for Linear-Elastic Plane-Starin Fracture Toughness KIc of Metallic Materials," American Society of Testing and Materials.

ATR, 2009, *Advanced Test Reactor National Scientific Users' Guide*, INL/EXT-08-14709, Idaho National Laboratory.

Busby, J. T., G. S Was, and E. A. Kenik, 2002, "Isolating the effect of radiation-induced segregation in irradiation- assisted stress corrosion cracking of austenitic stainless steels," *J. Nucl. Mater.*, 302, 1: 20-40.

Byun, T. and N. Hashimoto, 2006, "Strain Localization in Irradiated Materials", Nuclear Engineering and Technology, vol 38, N7: 619-638

Chateau, J. P., D. Delafosse, and T. Magnin, 2002a, "Numerical simulations of hydrogen–dislocation interactions in fcc stainless steels.: part I: hydrogen–dislocation interactions in bulk crystals," *Acta Materialia*, 50, 6: 1507-1522.

Chateau, J. P., D. Delafosse, and T. Magnin, 2002b, "Numerical simulations of hydrogen–dislocation interactions in fcc stainless steels.: part II: hydrogen effects on crack tip plasticity at a stress corrosion crack," *Acta Materialia*, 50, 6: 1523-1538.

Chopra O.K., A.S. Rao, 2011," A review of irradiation effects on LWR core internal materials – IASCC susceptibility and crack growth rates of austenitic stainless steels", Journal of Nuclear Materials 409 235-256

Connerman, J., R. Shogan, K. Fujimoto, T. Yonezawa, and Y. Yamaguchi, 2005, "Irradiation Effects in a Highly Irradiated Cold Worked Stainless Steel Removed from a Commercial PWR," *Proc. 12th International Conference on Environmental Degradation of Materials in Nuclear Power System – Water Reactors*, pp. 277–287.

Couvant T. et al. 2004 , "Effect of strain path on SCC of AISI 304L stainless steel in PWR primary environment at 360°C" , *Eurocorr'2004*, Nice, France, 2004).

Couvant T. et al. 2009, "Development of Understanding of the Interaction Between Localized Deformation and SCC of Austenitic Stainless Steels Exposed to Primary PWR Environment", *Proc. 14th International Conference on Environmental Degradation of Materials in Nuclear Power System – Water Reactors*, Virginia Beach, VA, 2009, pp. 182–194.

Couvant T. et al. 2011 " Strain Path Effect on IGSCC Initiation ad Oxidation of Alloy 182 Exposed to PWR Primary Water", *Proc. 15th International Conference on Environmental Degradation of Materials in Nuclear Power System – Water Reactors*, pp. 1631–1643.

Demma, A., 2010, "MRP-135," Revision 1, Electric Power Research Institute.

Demma, A., 2004, "MRP-121," Electric Power Research Institute.

Edwards, D. J., E. P Simonen, F. A. Garner, L. R. Greewood, B. M. Onliver, and S. M. Bruemmer, 2003, "Influence of irradiation temperature and dose gradients on the microstructura; evolution in neutron-irradiated 316 SS," *Nucl. Mater.,* 317: 32-45.

Edwards, D. J., F. A. Garner, S. M. Bruemmer, and Pal Efsing, 2009, "Nano-cavities observed in a 316SS PWR Flux Thimble Tube Irradiated to 33 and 70 dpa," *J. Nucl. Mater*., 384: 249–255.

Freyer, P. D., T. R. Mager, and M. A. Burke., 2007, "Hot Cell Crack Initiation Testing of Various Heats of Highly Irradiated 316 Stainless Steel Components Obtained from Three Commercial PWRs," *Proceedings of 13th International Conference on Environmental Degradation of Materials in Nuclear Power System – Water Reactors*.

Garner, F. A., E. P. Simonen, B. M. Oliver, L. R. Greenwood, M. L. Grossbeck, W. G. Wolfer, and P. M. Scott, 2006, "Retention of Hydrogen in FCC Metals Irradiated at Temperatures Leading to High Densities of Bubbles or Voids," *J. Nucl. Mater.*, 356: 122–135.

Girardin, G. and D. Delafosse, 2004, "Measurement of the saturated dislocation pinning force in hydrogenated nickel and nickel base alloys," *Scripta Materialia*, 51: 1177–1181.

Greenwood, L. R., F. A. Garner, B. M. Oliver, M. L. Grossbeck, and W. G. Wolfer, 2004, "Surprisingly Large Generation and Retention of Helium and Hydrogen in Pure Nickel Irradiated at High Temperatures and High Neutron Exposures," *Effects of Radiation on Materials*, ASTM STP 1447, M. L. Grossbeck, T. R. Allen, R. G. Lott, and A. S. Kumar, eds., ASTM International, West Conshohocken PA, 2004, pp. 529–539, *J. ASTM Int.* 1, 4, Paper ID JAI11365.

Gussev, M. N, P. Maksimkin, I. S. Osipov, and F. A Garner, 2009a, "Anomalously Large Deformation of 12Cr18Ni10Ti Austenitic Steel Irradiated to 55 dpa at 310 °C in the BN-350 Reactor," *J. Nucl. Mater.,* 386–388: 273–276.

Gussev, M. N, O. P. Maksimkin, I. S. Osipov, N. S. Silniagina, and F. A. Garner, 2009b, "Unusual Enhancement of Ductility Observed during Evolution of a 'Deformation Wave' in 12Cr18Ni10Ti Stainless Steel Irradiated in BN-350," *J. ASTM Int.*, 6, 7: paper ID JAI102062.

Hazelton, W. S. and W. H. Koo, 1988, NUREG-0313, Revision 2, U.S. Nuclear Regulatory Commission.

Horn, R. M., R. Hosler, P. Chou, and P. L. Andresen, 2013, "Studies of Crack Growth Rates in Irradiated Stainless Steel Control Blade Materials Tested in High Temperature Water," *16th Intl. Conf. on Environmental Degradation of Materials in Nuclear Power Systems – Water Reactors*, Asheville, NC.

Jensen, A., K. Gott, P. Efsing, and P. Anderson, 2003, "Crack Growth Behavior of Irradiated Type 304L Stainless Steel in Simulated BWR Environment," *11th Intl. Conf. on Environmental Degradation of Materials in Nuclear Power Systems – Water Reactors*.

Jensen, A., J. Stjarnsater, and R. Pathania, 2009, "Crack Growth Rate Testing of Fast Reactor Irradiated Type 304L and 316 SS in BWR and PWR Environments," *14th Int. Conf. on Environmental Degradation of Materials in Nuclear Power Systems*, Virginia Beach, VA.

Lian, T., 2013, EPRI Materials Degradation Matrix, Revision 3. EPRI, Palo Alto, CA. 3002000628

Magnin, T., C. Bosch, K. Wolski, and D. Delafosse, 2001, "Cyclic plastic deformation behaviour of Ni single crystals oriented for single slip as a function of hydrogen content," *Materials Science and Engineering: A*, 314, 1–2: 7-11.

Nakamura, T., M. Koshiishi, T. Torimaru, Y. Kitsunai, K. Takakura, K. Nakata, M. Ando, Y. Ishiyama, and A. Jensen, 2007, "Correlation between IASCC Growth Behavior and Plastic Zone Size of Crack Tip in 3.5 Neutron Irradiated Type 304L SS CT Specimen," *13th International Conference on Environmental Degradation of Materials in Nuclear Power Systems – Water Reactors*, Whistler, British Columbia.

Pathania, R., R. Carter, R. Horn, and P. Andresen, 2009, "Crack Growth Rates in Irradiated Stainless Steels in BWR Internals," *14th Intl. Conf. on Environmental Degradation of Materials in Nuclear Power Systems – Water Reactors*.

Rao A.S., 2009, NUREG/CR-7018

Rao A.S. , 2008, NUREG/CR-6965

Sumiya, R., S. Tanaka, K. Nakata, K. Takakura, M. Ando, T. Torimaru, and Y. Kitsunai, 2007, "K Validity Criterion of Neutron Irradiated Type 316L Stainless Steel CT Specimen for SCC Growth Test," *13th International Conference on Environmental Degradation of Materials in Nuclear Power Systems*, Whistler, British Columbia.

Takakura, K., K. Nakata, S. Tanaka, T. Nakamura, K. Chatani, and Y. Kaji, 2009, "Crack Growth Behavior of Neutron Irradiated L-Grade Austenitic Stainless Steels in Simulated BWR Conditions," *14th Intl. Conf. on Environmental Degradation of Materials in Nuclear Power Systems – Water Reactors*, Virginia Beach, VA.

Tang, H.T., 2003, *Materials Reliability Program: A Review of the Cooperative Irradiation Assisted Stress Corrosion Cracking Research Program (MRP-98),* EPRI, Palo Alto, CA. 1002807.

Tang, H.T., 2005, *Materials Reliability Program: PWR Internals Material Aging Degradation Mechanism Screening and Threshold Values (MRP-175).* EPRI, Palo Alto, CA. 1012081.

Tyler, C. R., P. E. Murray, and J. W. Nielsen, 2014, *CRADA EPRI Phase II Design Report*, Revision 1, INL/LTD-12-24400, Idaho National Laboratory.